2316 *Inorg. Chem.* **2010**, *49*, 2316–2324
DOI: 10.1021/ic9021992

Inorganic Chemistry
Article

Synthesis and Characterization of Three Ytterbium Coordination Polymers Featuring Various Cationic Species and a Luminescence Study of a Terbium Analogue With Open Channels

You-Wen Lin, Bo-Ren Jian, Sin-Chiang Huang, Chin-Her Huang, and Kuei-Fang Hsu*

Department of Chemistry, National Cheng Kung University, Tainan 701, Taiwan

Received November 6, 2009

Four novel metal-organic frameworks with 4,4′-oxybis(benzoate) (OBA) ligands and suitable cationic species, $[NH_3(CH_2)_2NH_3]_{0.5}[Yb(OBA)_2(H_2O)]$ (**1**), $(NH_4)[Yb(OBA)_2(H_2O)_2]$ (**2**), $Na[Yb(OBA)_2]\cdot 0.4DMF\cdot 1.5H_2O$ (**3**), and $Na[Tb(OBA)_2]\cdot 0.4DMF\cdot 1.5H_2O$ (**4**), have been synthesized and structurally characterized. The two-dimensional structure of **1** possesses open channels filled with ethylenediamine cations. The two-dimensional structure of **2** contains the network featuring organic ligands with uncoordinated functional RCO_2 groups suspended within the windows. The three-dimensional structure of **3**, in which Na^+ cations replaced the NH_4^+ cations of **2** and the presence of DMF molecules, adopts an open framework with large rhombic channels. The evacuated phase "$Na[Yb(OBA)_2]$" in **3** retained rigidity and crystallinity to a high temperature. Framework **4**, a terbium analogue of **3**, has the potential sensing ability; it exhibited gradually increasing luminescence intensities when dispersed sequentially in water, methanol, and ethanol as suspensions.

Introduction

The research of metal−organic frameworks (MOFs) including lanthanide ions has attracted much attention because of their abundant structural chemistry[1−9] and valuable optical[10−16] and magnetic[17−24] properties. The architectures of MOFs including the highly coordinated metal centers are often based on extended inorganic skeletons playing as building blocks, such as oxo- or carboxylato-bridged metal chains, which are exploited in the assemblage with suitable organic linkers carrying multiple carboxylate groups to generate porous and robust channels.[2,3,6,25−33] For example,

*To whom correspondence should be addressed. E-mail: hsukf@mail.ncku.edu.tw.

(1) Long, D. L.; Blake, A. J.; Champness, N. R.; Wilson, C.; Schröder, M. *Angew. Chem., Int. Ed.* **2001**, *40*, 2444.
(2) Dimos, A.; Tsaousis, D.; Michaelides, A.; Skoulika, S.; Golhen, S.; Ouahab, L.; Didierjean, C.; Aubry, A. *Chem. Mater.* **2002**, *14*, 2616.
(3) Pan, L.; Adams, K. M.; Hernandez, H. E.; Wang, X.; Zheng, C.; Hattori, Y.; Kaneko, K. *J. Am. Chem. Soc.* **2003**, *125*, 3062.
(4) Sun, Y. Q.; Zhang, J.; Chen, Y. M.; Yang, G. Y. *Angew. Chem., Int. Ed.* **2005**, *44*, 5814.
(5) Maji, T. K.; Mostafa, G.; Chang, H. C.; Kitagawa, S. *Chem. Commun.* **2005**, 2436.
(6) Devic, T.; Serre, C.; Audebrand, N.; Marrot, J.; Férey, G. *J. Am. Chem. Soc.* **2005**, *127*, 12788.
(7) Hoffart, D. J.; Leob, S. J. *Angew. Chem., Int. Ed.* **2005**, *44*, 901.
(8) Sun, Y. Q.; Zhang, J.; Yang, G. Y. *Chem. Commun.* **2006**, 1947.
(9) Luo, J.; Xu, H.; Liu, Y.; Zhao, Y.; Daemen, L. L.; Brown, C.; Timofeeva, T. V.; Ma, S.; Zhou, H. C. *J. Am. Chem. Soc.* **2008**, *130*, 9626.
(10) Serre, C.; Millange, F.; Thouvenot, C.; Gardant, N.; Pellé, F.; Férey, G. *J. Mater. Chem.* **2004**, *14*, 1540.
(11) Zhang, Z. H.; Okamura, T.; Hasegawa, Y.; Kawaguchi, H.; Kong, L. Y.; Sun, W. Y.; Ueyama, N. *Inorg. Chem.* **2005**, *44*, 6219.
(12) Huang, Y.; Wu, B.; Yuan, D.; Xu, Y.; Jiang, F.; Hong, M. *Inorg. Chem.* **2007**, *46*, 1171.
(13) Mahata, P.; Natarajan, S. *Inorg. Chem.* **2007**, *46*, 1250.
(14) de Lill, D. T.; de Bettencourt-Dias, A.; Cahill, C. L. *Inorg. Chem.* **2007**, *46*, 3960.
(15) Pham, B. T. N.; Lund, L. M.; Song, D. *Inorg. Chem.* **2008**, *47*, 6329.
(16) White, K. A.; Chengelis, D. A.; Zeller, M.; Geib, S. J.; Szakos, J.; Petoud, S.; Rosi, N. L. *Chem. Commun.* **2009**, 4506.
(17) Costes, J. P.; Clemente-Juan, J. M.; Dahan, F.; Nocodème, F.; Verelst, M. *Angew. Chem., Int. Ed.* **2002**, *41*, 323.
(18) Hatscher, S. T.; Urland, W. *Angew. Chem., Int. Ed.* **2003**, *42*, 2862.
(19) Hernández-Molina, M.; Ruiz-Pérez, C.; López, T.; Lloret, F.; Julve, M. *Inorg. Chem.* **2003**, *42*, 5456.
(20) He, Z.; Gao, E. Q.; Wang, Z. M.; Yan, C. H.; Kurmoo, M. *Inorg. Chem.* **2005**, *44*, 862.
(21) Manna, S. C.; Zangrando, E.; Bencini, A.; Benelli, C.; Chaudhuri, N. R. *Inorg. Chem.* **2006**, *45*, 9114.
(22) Cañadillas-Delgado, L.; Pasán, J.; Fabelo, O.; Hernández-Molina, M.; Lloret, F.; Julve, M.; Ruiz-Pérez, C. *Inorg. Chem.* **2006**, *45*, 10585.
(23) Fellah, F. Z. C.; Costes, J. P.; Dahan, F.; Duhayon, C.; Novitchi, G.; Tuchagues, J. P.; Vendier, L. *Inorg. Chem.* **2008**, *47*, 6444.
(24) Liu, H. C.; Chen, I. H.; Huang, A.; Huang, S. C.; Hsu, K. F. *Dalton Trans.* **2009**, 3447.
(25) Kiritsis, V.; Michaelides, A.; Skoulika, S.; Golhen, S.; Ouahab, L. *Inorg. Chem.* **1998**, *37*, 3407.
(26) Serpaggi, F.; Férey, G. *J. Mater. Chem.* **1998**, *8*, 2737.
(27) Reineke, T. M.; Eddaoudi, M.; O'Keeffe, M.; Yaghi, O. M. *Angew. Chem., Int. Ed.* **1999**, *38*, 2590.
(28) Reineke, T. M.; Eddaoudi, M.; Fehr, M.; Douglas, K.; Yaghi, O. M. *J. Am. Chem. Soc.* **1999**, *121*, 1651.
(29) Pan, L.; Zheng, N.; Wu, Y.; Han, S.; Yang, R.; Huang, X.; Li, J. *Inorg. Chem.* **2001**, *40*, 828.
(30) de Lill, D. T.; Gunning, N. S.; Cahill, C. L. *Inorg. Chem.* **2005**, *44*, 258.
(31) Guo, X.; Zhu, G.; Fang, Q.; Xue, M.; Tian, G.; Sun, J.; Li, X.; Qiu, S. *Inorg. Chem.* **2005**, *44*, 3850.
(32) Rosi, N. L.; Kim, J.; Eddaoudi, M.; Chen, B.; O'Keeffe, M.; Yaghi, O. M. *J. Am. Chem. Soc.* **2005**, *127*, 1504.

 Published on Web 02/01/2010

Table 1. Crystal Data for **1**−**4**

	1	**2**	**3**	**4**
formula	$C_{29}H_{23}NO_{11}Yb$	$C_{28}H_{24}NO_{12}Yb$	$C_{28}H_{16}O_{10}YbNa$	$C_{28}H_{16}O_{10}TbNa$
formula weight	734.5	739.5	708.4	750.6
crystal system	triclinic	orthorhombic	orthorhombic	Orthorhombic
space group	$P\bar{1}$	*Pbca*	$Cmc2_1$	$Cmc2_1$
a (Å)	9.5795(2)	9.9772(6)	26.800(3)	26.920(1)
b (Å)	10.4344(2)	19.1646(12)	14.933(2)	15.1196(5)
c (Å)	14.6343(3)	28.2445(18)	7.1681(7)	7.2696(3)
α (deg)	71.945(1)	90	90	90
β (deg)	76.259(1)	90	90	90
γ (deg)	88.254(1)	90	90	90
V (Å^3)	1349.5(1)	5400.6(6)	2868.7(5)	2958.9(2)
Z	1	8	4	4
ρ_{calcd} (g cm^{-3})	1.808	1.819	1.622	1.559
μ (mm^{-1})	3.531	3.532	3.328	2.457
T (K)	293	293	293	293
total reflections	29197	38227	11433	11415
unique reflections (R_{int})	12963 (0.0578)	6731 (0.0543)	3762 (0.0289)	3732 (0.0280)
goodness-of-fit	0.922	1.019	0.966	1.178
R_1[a] [$I > 2\sigma(I)$]	0.0280	0.0348	0.0494	0.0515
wR_2[b] [$I > 2\sigma(I)$]	0.0555	0.0853	0.1494	0.1579

[a] $R_1 = \sum||F_o| - |F_c||/\sum|F_o|$. [b] $wR_2 = \{\sum w(F_o^2 - F_c^2)^2/\sum w(F_o^2)^2\}^{1/2}$.

Table 2. Selected Bond Length (Å) for **1**−**4**

		1	
Yb(1)−O(6)	2.170(2)	Yb(1)−O(11)$_w$	2.300(2)
Yb(1)−O(1)	2.182(2)	Yb(1)−O(10A)[c]	2.389(2)
Yb(1)−O(7A)[a]	2.224(2)	Yb(1)−O(9A)[c]	2.390(2)
Yb(1)−O(5A)[b]	2.228(2)		
		2	
Yb(1)−O(7A)[d]	2.160(2)	Yb(1)−O(11)$_w$	2.317(3)
Yb(1)−O(5A)[e]	2.169(3)	Yb(1)−O(2)	2.375(3)
Yb(1)−O(6)	2.250(2)	Yb(1)−O(1)	2.388(2)
Yb(1)−O(12)$_w$	2.275(3)		
		3	
Yb(1)−O(4A)[f]	2.223(7)	Yb(1)−O(1)	2.370(8)
Yb(1)−O(4B)[g]	2.223(7)	Yb(1)−O(1A)[j]	2.370(8)
Yb(1)−O(5A)[h]	2.322(7)	Yb(1)−O(2)	2.390(8)
Yb(1)−O(5B)[i]	2.322(7)	Yb(1)−O(2A)[j]	2.390(8)
		4	
Tb(1)−O(4A)[f]	2.281(6)	Tb(1)−O(1)	2.417(6)
Tb(1)−O(4B)[g]	2.281(6)	Tb(1)−O(1A)[j]	2.417(6)
Tb(1)−O(5A)[h]	2.360(7)	Tb(1)−O(2)	2.470(7)
Tb(1)−O(5B)[i]	2.360(7)	Tb(1)−O(2A)[j]	2.470(7)

[a] $-x+1, -y+1, -z+1$. [b] $-x+1, -y+1, -z+2$. [c] $-x+2, -y+2, -z$. [d] $-x, -y, 1-z$. [e] $x, 1/2-y, 1/2+z$. [f] $1/2-x, -1/2+y, z$. [g] $1/2+x, -1/2+y, z$. [h] $1/2-x, 1/2-y, -1/2+z$. [i] $1/2+x, 1/2-y, -1/2+z$. [j] $1-x, y, z$.

the assembly of 4,4′-biphenyldicarboxylate (BPDC) units with metal ions has led to the construction of frameworks containing large rhombic channels (ca. 2 nm) in the structure $Tb_2(BPCD)_3(H_2O)_2 \cdot DMF$.[31] The framework formed from 1,3,5-benzenetrisbenzoate (BTB) exhibits unique open hexagonal channels (ca. 1 nm); the evacuated solid "Tb(BTB)" displayed structural ordering and a high surface area upon guest removal.[6] Such porous MOFs containing europium or terbium centers have recently been demonstrated to recognize

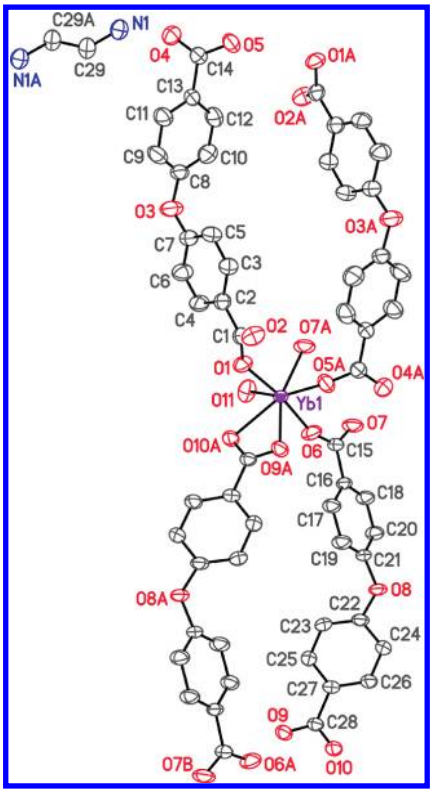

Figure 1. ORTEP representations of the partial linkage motifs in **1**. Thermal ellipsoids are presented at the 50% probability level.

a variety of guest ions and molecules through luminescence studies.[28,34−39] The evacuated solid $Tb_2(BDC)_3$ (BDC: 1,4-benzenedicarboxylate) was an early reported framework for

(33) Guo, X.; Zhu, G.; Sun, F.; Li, Z.; Zhao, X.; Li, X. *Inorg. Chem.* **2006**, *45*, 2581.
(34) Liu, W.; Jiao, T.; Li, Y.; Liu, Q.; Tan, M.; Wang, H.; Wang, L. *J. Am. Chem. Soc.* **2004**, *126*, 2280.
(35) Zhao, B.; Chen, X. Y.; Cheng, P.; Liao, D. Z.; Yan, S. P.; Jiang, Z. H. *J. Am. Chem. Soc.* **2004**, *126*, 15394.
(36) Wong, K. L.; Law, G. L.; Yang, Y. Y.; Wong, W. T. *Adv. Mater.* **2006**, *18*, 1051.
(37) Chen, B.; Yang, Y.; Zapata, F.; Lin, G.; Qian, G.; Lobkovsky, E. B. *Adv. Mater.* **2007**, *19*, 1693.
(38) Harbuzaru, B. V.; Corma, A.; Rey, F.; Atienzar, P.; Jordá, J. L.; García, H.; Ananias, D.; Carlos, L. D.; Rocha, J. *Angew. Chem., Int. Ed.* **2008**, *47*, 1080.
(39) Chen, B.; Wang, L.; Zapata, F.; Qian, G.; Lobkovsky, E. B. *J. Am. Chem. Soc.* **2008**, *130*, 6718.

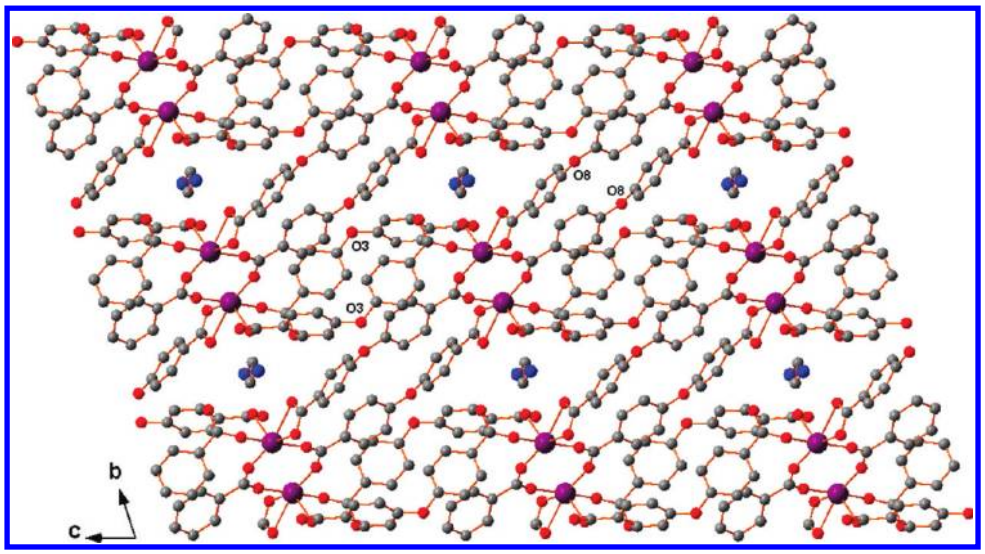

Figure 2. Network parallel to the *bc* plane in **1**. Color scheme: Yb atoms, purple; C atoms, gray; O atoms, red; N atoms, blue.

the detection of small molecules, which, when encapsulated within its channels, exhibited quenching of its luminescence through the action of N−H and O−H oscillators.[28] In addition, the evacuated solid Eu(BTC) (BTC: 1,3,5-benzenetricarboxylate) possessing larger tubular channels (6.8 × 6.8 Å) was able to sense solvents acetone and dimethylformamide (DMF), mediated by significant decreases and increases in luminescence intensity, respectively.[36]

In this paper, we report three new structures of ytterbium-organic frameworks prepared from 4,4′-oxybis(benzoate) ligands (OBA) precipitated with versatile cationic species; their formulas can be expressed as $A[Yb(OBA)_2(H_2O)_n]\cdot L$ (where A is $[NH_3(CH_2)_2NH_3]_{0.5}$ for **1**, NH_4 for **2**, and Na for **3**, and L denotes H_2O and DMF molecules). The OBA ligand provides multiple chelating modes and a flexible ether oxygen atom to direct the formation of MOFs with diverse phases.[40−45] For example, a series of manganese-based MOFs featuring this ligand has been derived by varying the synthetic parameters, such as the reaction temperature and time.[43] To the best of our knowledge, two-dimensional structures of the types $[Zn_2(OBA)_2(DMF)_2]\cdot L$[40] and $[Cu_2(OBA)_2(DMF)(C_2H_5OH)]\cdot L$[45] are the only examples possessing open channels constructed from OBA ligands only. In this present study, the structure for **3** is a rare three-dimensional framework, exhibiting large rhombic channels, fabricated from lanthanide one-dimensional skeletons and OBA ligands. We also observed this phase for the terbium analogue **4**. Herein, we describe the synthesis and structural characterization of the three phases in **1**−**3** and a luminescence study for framework **4**.

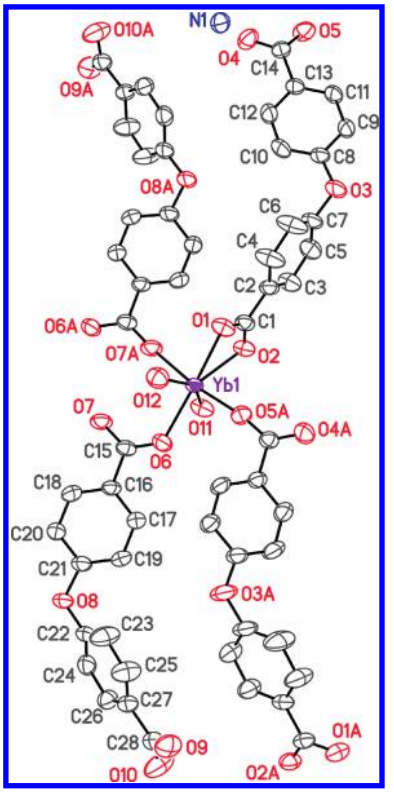

Figure 3. ORTEP representations of the partial linkage motif in **2**. Thermal ellipsoids are presented at the 50% probability level.

Experimental Section

All chemicals were purchased from Aldrich and used as received. Elemental analyses (EA) were performed using an Elemental vario EL III analyzer. Fourier transform infrared (FTIR) spectra were measured from KBr pellets using a Perkin−Elmer Spectrum RX1 FTIR spectrometer. Powder X-ray analyses were performed using a Shimadzu XRD-7000s X-ray diffractometer. Thermogravimetric and differential thermal analyses (TGA/DTA) were performed on powder samples in flowing N_2 gas using a Shimadzu DTG-60 analyzer operated at a heating rate of 10 °C/min. Luminescence spectra were recorded using a Hitachi 4500 spectrometer with the photomultiplier tube voltage 400 V, the scan speed 1200 nm/min, and the slit width 5 nm. The absorption spectra were recorded using a Hitachi U-4100 spectrophotometer with the photomultiplier tube voltage 230 V, the scan speed 300 nm/min, and the slit width 1 nm.

(40) Kondo, M.; Irie, Y.; Shimizu, Y.; Miyazawa, M.; Kawaguchi, H.; Nakamura, A.; Naito, T.; Maeda, K.; Uchida, F. *Inorg. Chem.* **2004**, *43*, 6139.
(41) Sun, C. Y.; Gao, S.; Jin, L. P. *Eur. J. Inorg. Chem.* **2006**, 2411.
(42) Mahata, P.; Sundaresan, A.; Natarajan, S. *Chem. Commun.* **2007**, 4471.
(43) Mahata, P.; Prabu, M.; Natarajan, S. *Inorg. Chem.* **2008**, *47*, 8451.
(44) Martin, D. P.; Staples, R. J.; LaDuca, R. L. *Inorg. Chem.* **2008**, *47*, 9754.
(45) Xue, D. X.; Lin, J. B.; Zhang, J. P.; Chen, X. M. *CrystEngComm* **2009**, *11*, 183.

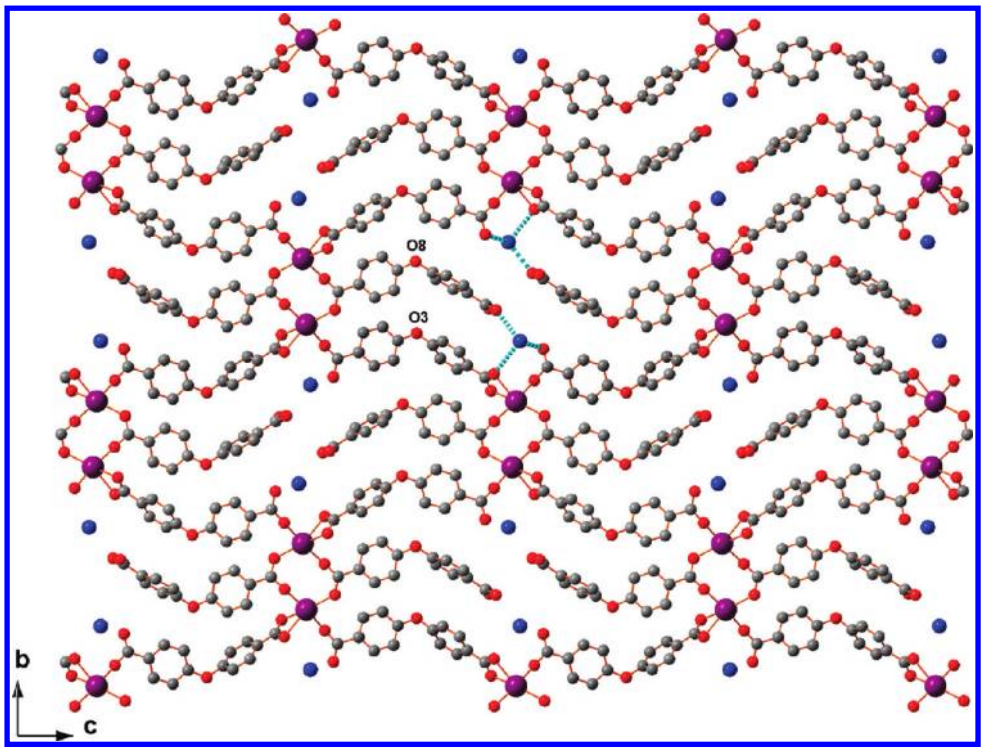

Figure 4. Network parallel to the *bc* plane in **2**. Color scheme: Yb atoms, purple; C atoms, gray; O atoms, red; N atoms, blue. Dashed lines represent hydrogen bonds between the ammonium nitrogen atoms and oxygen atoms of the carboxylate groups.

$[NH_3(CH_2)_2NH_3]_{0.5}[Yb(OBA)_2(H_2O)]$ (1). $Yb(NO_3)_3 \cdot 5H_2O$ (0.20 mmol) and H_2OBA (0.20 mmol) were added to a mixture of H_2O (10.0 mL) and 1,2-diaminoethane (99.9%, 1.3 mL), the pH of which had been adjusted to about 4.2 through the addition of HCl. The mixture was heated in a 23 mL Teflon-lined autoclave at 150 °C for 3 days and then slowly cooled to 50 °C. Colorless plate crystals of **1** were obtained in the final product (yield: ca. 40%, based on H_2OBA). Calcd for $C_{29}H_{23}NO_{11}Yb$ (734.5): C, 47.42; H, 3.16; N, 1.91. Found: C, 47.46; H, 3.15; N, 1.88. IR bands (cm^{-1}): 3450 mbr(O−H), 3070 m(C−H), 1679 s(C═O), 1590 s(C═C), 1413 s(C═C), 1276 s(C−O), 1155 s(C−O), 860 m and 764 $m(C-H)_{oop}$.

$(NH_4)[Yb(OBA)_2(H_2O)_2]$ (2). $Yb(NO_3)_3 \cdot 5H_2O$ (0.20 mmol) and H_2OBA (0.20 mmol) were added to a mixture of $(NH_4)_2SO_4$ (1 M, 10.0 mL) and $(CH_3)_4NOH$ (25%, 1.8 mL), the pH of which had been adjusted to about 6.9. The mixture was heated in a 23 mL Teflon-lined autoclave at 150 °C for 3 days and then slowly cooled to 50 °C. Colorless lamellar crystals of **2** were obtained in the final product (yield: ca. 40%, based on H_2OBA). Calcd for $C_{28}H_{24}NO_{12}Yb$ (739.5): C, 45.48; H, 3.27; N, 1.89. Found: C, 45.19; H, 3.22; N, 1.81. IR bands (cm^{-1}): 3325 mbr(O−H), 3071 m(C−H), 1689 s(C═O), 1591 s(C═C), 1482 s(C═C), 1247 s-(C−O), 1157 m(C−O), 857 m and 768 $m(C-H)_{oop}$.

$Na[Yb(OBA)_2] \cdot 0.4DMF \cdot 1.5H_2O$ (3). $Yb(NO_3)_3 \cdot 5H_2O$ (0.50 mmol), H_2OBA (1.00 mmol), and NaCl (0.50 mmol) were added to a mixture of DMF (6.0 mL) and ethanol (6.0 mL), the pH of which had been adjusted to about 6.0 by 5 M NaOH. The mixture was heated in a 23 mL Teflon-lined autoclave at 150 °C for 3 days and then slowly cooled to 50 °C. Colorless needlelike crystals of **3** were obtained in the final product (yield: 93%, based on H_2OBA). Calcd for $C_{29.2}H_{21.8}N_{0.4}O_{11.9}YbNa$ (764.7): C, 45.86; H, 2.87; N, 0.73. Found: C, 44.89; H, 2.82; N, 0.72. IR bands (cm^{-1}): 3516 mbr(O−H), 3261 m(C−H), 1649 m(C═O), 1590 s(C═C), 1524 $s(N-H)_{bend}$, 1413 s(C═C), 1251 s(C−O), 1163 m(C−O), 875 m and 779 $m(CH)_{oop}$.

$Na[Tb(OBA)_2] \cdot 0.4DMF \cdot 1.5H_2O$ (4). $Tb(NO_3)_3 \cdot 6H_2O$ (0.5 mmol), H_2OBA (1.0 mmol), and NaCl (0.5 mmol) were added to a mixture of DMF (6.0 mL) and ethanol (6.0 mL). The mixture was heated in a 23 mL Teflon-lined autoclave at 150 °C for 3 days and then slowly cooled to 50 °C. Light-yellow needlelike crystals of **4** were obtained in the final product (yield: 96%, based on H_2OBA). Calcd for $C_{29.2}H_{21.8}N_{0.4}O_{11.9}TbNa$ (750.6): C, 46.73; H, 2.93; N, 0.75. Found: C, 43.76; H, 2.90; N, 0.85. IR bands (cm^{-1}): 3586 mbr(O−H), 3173 m(C−H), 1635 m(C═O), 1598 s(C═C), 1524 $s(N-H)_{bend}$, 1413 s(C═C), 1251 s(C−O), 1155 m(C−O), 882 m and 780 $m(CH)_{oop}$.

Single-Crystal X-ray Structural Analyses. Single crystals of compounds **1**−**4** were selected for indexing and data collection on a Bruker APEXII CCD diffractometer, irradiating with graphite-monochromated Mo Kα radiation (λ = 0.71073 Å). Data integrations and absorption corrections were processed using the SAINT and SADABS functions in the APEX2 package, respectively.[46] The structures were solved and refined using the SHELXTL-97 package.[47] For **1**, the space group was initially determined to be *P*1. All the non-hydrogen atoms were easily located using the Direct method, followed with anisotropic refinements. Examination by ADDSYMM in the PLATON package, however, suggested the existence of an inversion center.[48] Using the *P*1 space group led to severe correlations of the thermal parameters or fractional coordinates for a couple of atoms. The Patterson method was successfully applied, through the location of heavy ytterbium atom, to solve crystal **1** with the space group $P\bar{1}$. The remaining atoms were found successively from Fourier difference maps. All the non-hydrogen atoms were refined anisotropically without the appearance of large correlation matrix elements again. The hydrogen atoms of OBA ligands were calculated with the riding model. The hydrogen atoms for the NH_3 group of cationic ethylenediamine were located from Fourier difference maps, but the atoms

(46) *APEX*, version 2008.2-0; Bruker Analytical X-ray Systems: Madison, WI, 2006.

(47) Sheldrick, G. M. *SHELXTL-Plus, NT crystallographic system*, version 6.1; Bruker Analytical X-ray Systems: Madison, WI, 2000.

(48) Spek, A. L. *PLATON, A Multipurpose Crystallographic Tool*; Utrecht University: Utrecht, The Netherlands, 1999.

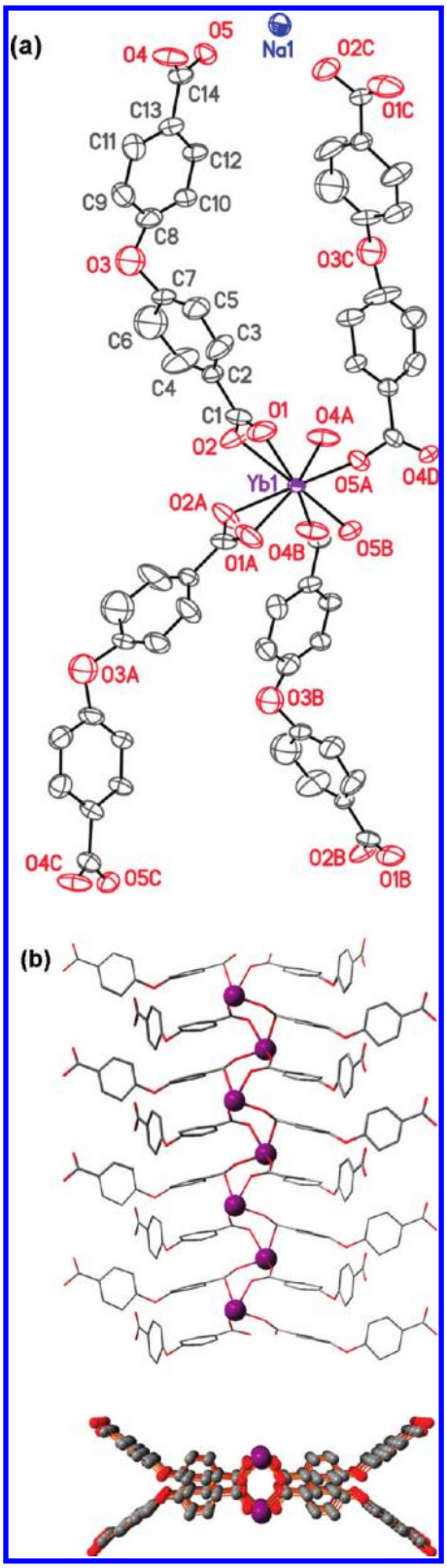

Figure 5. (a) ORTEP representations of the partial linkage motif in **3**. Thermal ellipsoids are presented at the 35% probability level. (b) $Yb1^{3+}$ ions extending into an infinite chain via OBA3 ligands under a 2_1 translation along the *c* axis. Perspective view of the infinite chains along the *c* axis. Color scheme: Yb atoms, purple; C atoms, gray; O atoms, red.

attached to the $(CH_2)_2$ group could not be located or calculated geometrically. The final cycle of refinement converged at $R_1 = 0.0280$ and $wR_2 = 0.0555$.

For **2**, the space group was determined to be *Pbca* based on statistics of intensity distribution and systematic absences of structure factors. All the non-hydrogen atoms were located on the electron density maps and refined anisotropically. The hydrogen atoms of OBA ligands were calculated with the riding model while the atoms of NH_4^+ catons were located from Fourier difference maps. The final cycle of refinement converged at values of R_1 and wR_2 of 0.0348 and 0.0853, respectively.

For **3**, the space group was determined to be $Cmc2_1$. The Direct method was used to locate the ytterbium and sodium atoms with the remaining atoms being found in Fourier difference maps. The DFIX instruction was applied to constrain several C−O and C−C bonds for the OBA ligand, which possessed high degrees of freedom in this structure. Crystal **3** contained DMF and H_2O lattice molecules encapsulated with the channels, as characterized by elemental and thermogravimetric analyses. These atoms could not be located on Fourier difference maps. The SQUEEZE function in the PLATON package was then applied to remove the unresolved electron density, thereby improving the final cycle of refinement, converging at values of R_1 and wR_2 of 0.0494 and 0.1494, respectively. An alert "A" for a solvent accessible void in this structure, provided by the checkCIF program, arose when ignoring these unresolved severely disordered molecules. All the located non-hydrogen atoms were refined anisotropically except two atoms: oxo-bridged O3 and C6. The Tb analogue **4** crystallized in the same structure. The DFIX instruction was applied to constrain the similar C−O and C−C bonds for the flexible OBA ligand. The SQUEEZE function was also applied to remove the residual electron densities from the unlocated lattice molecules (note that the checkCif report provided the same alert for **3** as a result of this operation). The final cycle of refinement, including all the non-hydrogen atoms refined anisotropically, converged at values of R_1 and wR_2 of 0.0515 and 0.1579, respectively. The hydrogen atoms of the OBA ligands in **3** and **4** were calculated geometrically. Crystallographic data for **1**−**4** are summarized in Table 1; selected bond lengths for **1**−**4** are listed in Table 2.

Results and Discussion

Compound $[NH_3(CH_2)_2NH_3]_{0.5}[Yb(OBA)_2(H_2O)]$ (**1**) features a new two-dimensional structure. The partial linkage motif of the network reveals that one Yb1 ion is coordinated to seven oxygen atoms, contributed from two OBA3 and three OBA8 ligands (named in terms of the numeric number label of the oxo-bridging atom) and one water molecule (Figure 1). The Yb1−O distances are ranged from 2.170(2) to 2.390(2) Å. The two OBA3 ligands coordinate in a monodentate manner to the Yb1 ion through the μ_1-carboxylato-κ^1O1 and -κ^1O5 groups. One of the OBA8 ligands chelates the Yb1 ion through the μ_1-carboxylato-κ^2O9,O10 group, while other two bridge the inversion-related Yb1 ions into a dimeric unit through the μ_2-carboxylato-κ^2O6:O7 groups. The unit formed with an Yb···Yb distance of 5.049 Å is surrounded by four pairs of ligands that extend into the network in **1** (Figure 2). The network possesses slightly compressed rhombic windows, which stack parallel along the *a* axis to form open channels with the $NH_3(CH_2)_2NH_3^{2+}$ cations distributed inside. The TGA curve of **1** (Supporting Information, Figure S1) exhibited a weight loss between 190 and 240 °C corresponding to the dissociation of coordinated H_2O molecules (calcd 2.45%; found 2.50%). However, as revealed by the continuous steps of weight losses since 240 °C, the further evaporation of cationic species led to the decomposition of the network.

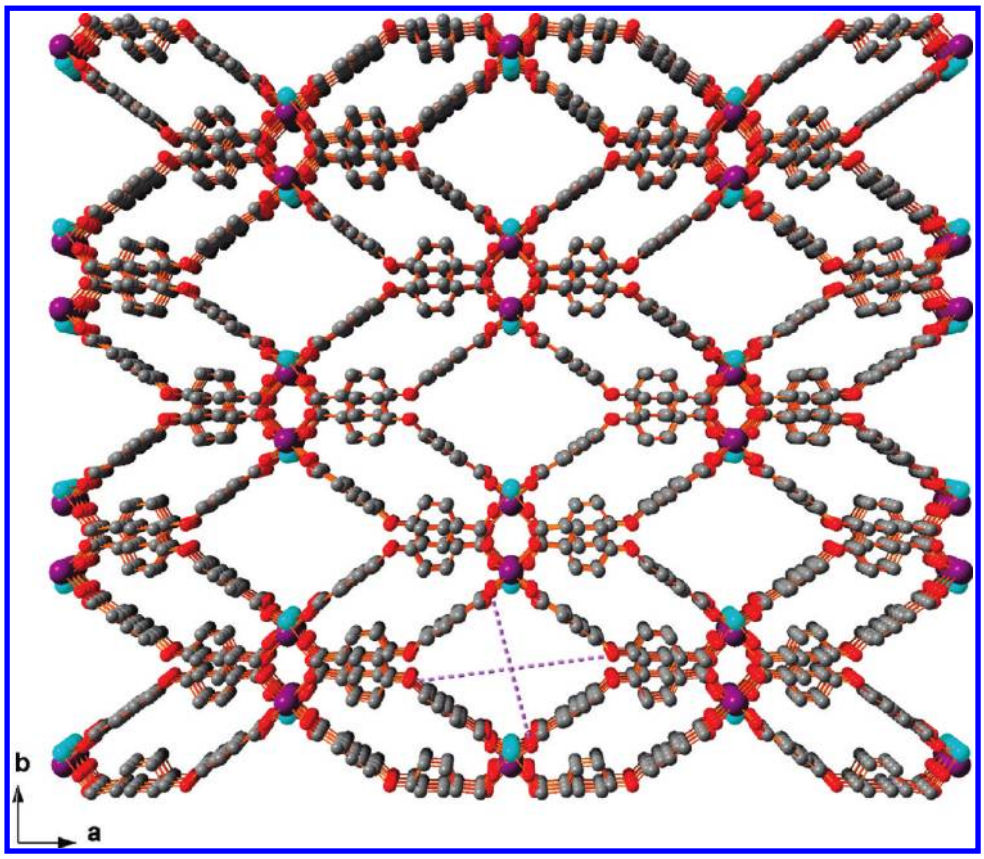

Figure 6. Perspective view of the framework along the *c* axis in **3**. Color scheme: Yb atoms, purple; C atoms, gray; O atoms, red; Na atoms, cyan. The dimensions of the channels were measured by in terms of the O···O distance, less one oxygen aom diameter (2.6 Å).

Compound $(NH_4)[Yb(OBA)_2(H_2O)_2]$ (**2**) possesses a new two-dimensional structure, in which the asymmetric unit contains one Yb1 ion, two crystallographic OBA3 and OBA8 ligands, two water molecules, and one ammonium cation (Figure 3). The Yb1 ion is seven-coordinated with the Yb1−O distances distributed over the range 2.160(2)−2.388(3) Å. The OBA3 ligands coordinate the Yb1 ion through the μ_1-carboxylato-κ^2O1,O2 and -κ^1O5 groups. The OBA8 ligands bridge the Yb1 ions into a dimeric unit through their μ_2-carboxylato-κ^2O6:O7 groups. The dimeric units, featuring a Yb···Yb distance of 4.761 Å, are then joined together through the ligands to form the network in **2** (Figure 4). Within the network, the OBA8 ligands have their terminal $-CO_2$ groups suspended around the centers of open rings. Several MOFs carrying exposed carboxylate, formate, or amino groups have been described previously; frameworks featuring organic ligands with presenting dangling functional groups within the channels should exhibit molecular recognition ability and chemical reactivity.[49,50] The OBA8 ligands with the terminal carboxylate groups are not exposed, however, in **2** because of translational stacking of the network along the *a* axis. The NH_4^+ cations participated in hydrogen bonding with the oxygen atoms of the carboxylate groups within the network.[51] We suspected that the creation of a more polar bonding environment by using Na^+ cations might induce a different structural topology. Indeed, we discovered such a prospective third phase for $Na[Yb(OBA)_2]\cdot 0.4DMF\cdot 1.5H_2O$ (**3**). The TGA curve of **2** (Supporting Information, Figure S1) displayed a weight loss between 150 and 200 °C corresponding to the dissociation of coordinated H_2O molecules (calcd 4.87%; found 4.91%). The continued removal of cationic species could be associated with the cleavage of carboxylate groups of organic ligands to have the evaporation of one NH_3 and H_2O and two CO_2 molecules (calcd 16.63%; found 16.78%) in the second step of weight loss between 200 and 400 °C. All the hydrocarbon species were evaporated in the third step of weight loss from 400 to 600 °C.

Structure **3** adopts a new three-dimensional framework, in which the asymmetric unit contains an eight-coordinated Yb1 ion, one OBA3 ligand, and one Na1 cation (Figure 5a). The Yb1−O distances are distributed within the range 2.223(7)−2.390(8) Å, with oxygen atoms contributed from six OBA ligands. The μ_2-carboxylato-κ^2O4:O5 groups of the OBA3 ligands extend the Yb1 ions into an infinite chain along the *c* axis, where the ytterbium atoms are separated by a distance of 5.404 Å (Figure 5b). From another point of view, these organic ligands circulate along the chain through a 2_1 symmetric translation, with their end μ_1-carboxylato-κ^2O1, O2 groups responsible for linking neighboring chains. A framework possessing open rhombic channels is then present in **3**, where the Na^+ cations are embedded at the periphery of the chains, stabilized by Na−O distances ranging between 2.207 and 2.319 Å (Figure 6). The OBA3 ligands are bent to

(49) Zhu, J.; Bu, X.; Feng, P.; Stucky, G. D. *J. Am. Chem. Soc.* **2000**, *122*, 11563.

(50) Vaidhyanathan, R.; Natarajan, S.; Rao, C. N. R. *Inorg. Chem.* **2002**, *41*, 4496.

(51) Hydrogen bonding between ammonium cations and oxygen atoms was evident from the N···O and H···O distances and the N−H···O angles. For the O10, O4, O1, and O2 atoms, the N···O distances were 2.650, 2.811, 2.828, and 2.883 Å, respectively, the H···O distances were 1.767, 1.823, 2.006, and 2.061 Å, respectively, and the N−H···O angles were 146.2.0, 164.0, 150.5, and 173.4°, respectively.

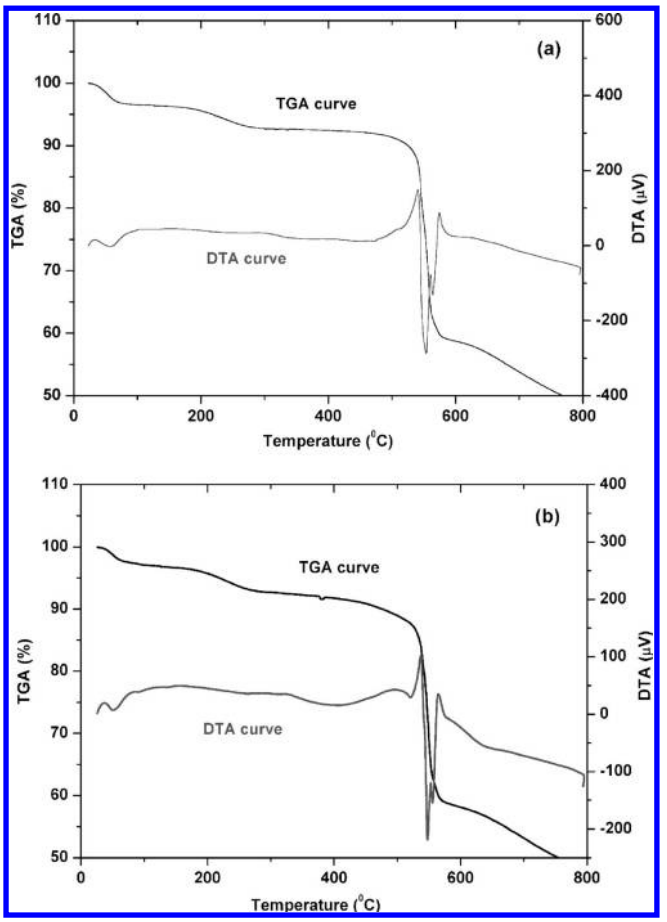

Figure 7. TG/DTA curves for (a) $Na[Yb(OBA)_2]\cdot 0.4DMF\cdot 1.5H_2O$ (**3**) and (b) $Na[Tb(OBA)_2]\cdot 0.4DMF\cdot 1.5H_2O$ (**4**).

113.4° at their ether-oxygen atom (C−O−C sites) to shrink the sizes of the windows of the channels having dimensions about 10.2 × 7.6 Å (minimum O···O distance less one O diameter of 2.6 Å). In the previous two networks, the OBA ligands were more stretchable, with C−O−C angles distributed between 118.1° and 123.4°.

The lattice H_2O and DMF molecules are distributed within the rhombic channels; we estimated their contents from elemental analyses and TGA. The TGA curve of $Na[Yb(OBA)_2]\cdot 0.4DMF\cdot 1.5H_2O$ (**3**) revealed (Figure 7a) weight losses between 30 and 120 °C, corresponding to $1.5H_2O$ molecules (calcd 3.53%; found 3.55%), and between 120 and 320 °C, corresponding to 0.4DMF molecules (calcd 3.82%; found 3.86%). The TGA curve indicated that the evacuated framework of "$Na[Yb(OBA)_2]$" was thermally sustained up to a temperature of about 500 °C. In the DTA curve, a small endothermic peak at 56 °C resulted from the loss of H_2O molecules, while a large peak at 555 °C resulted from the collapse of the framework. The comparative powder X-ray diffraction (PXRD) patterns revealed that, after treatment at 250 °C for 12 h under vacuum, the sample retained the high crystallinity found in the original phase **3** (Supporting Information, Figure S2). We suspect that the inorganic Na^+ cations coordinated to oxygen atoms around the surface of channels play an important factor in maintaining the structural ordering of this evacuated framework. The use of smaller Li^+ cations to investigate if this framework could be sustained by the reaction gave a uniform microcrystalline solid. The PXRD pattern (Supporting Information, Figure S3) revealed the solid crystallized in a different phase from that in **3**. (These crystals were unfortunately too tiny for the single-crystal structural characterization.)

In the syntheses, a range of cations, $NH_4(CH_2)_2NH_4^{2+}$, NH_4^+ and Na^+, has been selected to participate in the fabrication of three different structural topologies with Yb ions and OBA ligands successfully. We noted that some solvent present in the reaction was essential to favor the phase precipitated with the cationic template. The phase **1** was simply synthesized in the aqueous solution under a mild hydrothermal condition. For preparing the phase **2**, the aqueous solution without the presence of $(CH_3)_4NOH$ led to the formation of a condensed 3D framework $Yb_2(OBA)_3(H_2O)_4$[52] (Supporting Information, Figure S4). Interestingly, this condensed framework rather than a porous framework **3** was formed when DMF was absent in the solution. In the mixed DMF/EtOH or DMF/H_2O solution, the phase **3** was synthesized by the stoichiometric ratio of sodium, ytterbium and OBA components from starting chemicals that produced a high yield of compound. (The use of EtOH solvent improved the size of growing crystals provided for the structural characterization.). The reactions with the stoichiometric ratio of composition tried to improve the low yields of compounds **1** and **2** failed because the two phases were not formed under such a condition.

The Tb analogue $Na[Tb(OBA)_2]\cdot 0.4DMF\cdot 1.5H_2O$ (**4**) crystallizes in the same structure as that in **3**; its asymmetric unit contains an eight-coordinated Tb1 ion, one OBA3 ligand, and one Na1 cation (Supporting Information, Figure S5). The Tb1−O distances are distributed within the range 2.281(6)−2.470(7) Å. The solid luminescence of **4** exhibits four emission bands, with maxima at 490, 545, 584, and 622 nm, corresponding to the characteristic transitions between the excited state $^5D_4$ and the ground multiplets ^7F_J (J = 3−6), respectively (Figure 8a). The excitation band of **4** displays one peak maximum centered at 295 nm with a broad shoulder to its left. We examined the ligand using H_2OBA, which displays luminescence at 320 nm (Figure 8b).[53] The excitation band of H_2OBA, which spanned the near-ultraviolet region (200−300 nm), mimics the excitation band of **4**, providing the basis for the ligand to sensitize Tb^{3+} ions.[54,55] The solid H_2OBA displays a broad absorption band located in a similar region (Supporting Information, Figure S6). The ligand-based emission was quenched in the luminescence spectrum of **4**, further supporting the notion of a ligand-to-metal energy transfer process (Supporting Information, Figure S7). The TG/DTA curves of **4** revealed that the evacuated solid of "$Na[Tb(OBA)_2]$" maintained its stability at high temperatures (Figure 7b).[56] The stronger luminescence

(52) Crystal data for $Yb_2(OBA)_3(H_2O)_4$: triclinic $P\bar{1}$, a = 9.2118(8), b = 14.772(1), c = 28.637(2) Å, V = 3842.4(6) Å^3, Z = 2, ρ = 2.038 g cm^{-3}, μ = 4.926 mm^{-1}, T = 220 K, 46523 total reflections, 18876 unique reflections (R_{int} = 0.0398), R_1 = 0.0485 [$I > 2\sigma(I)$], $wR2$ = 0.1140 [$I > 2\sigma(I)$]. The $Tb_2(OBA_3)(H_2O)_4$ featuring a 2D network was reported in the literature, which symmetry crystallized in monoclinic $P2/c$ .Liu, G. F.; Qiao, Z. P.; Wang, H. Z.; Chen, X. M.; Yang, G. *New. J. Chem.* **2002**, *26*, 791.

(53) Tao, J.; Shi, J. X.; Tong, M. L.; Zhang, X. X.; Chen, X. M. *Inorg. Chem.* **2001**, *40*, 6328.

(54) Richardson, F. S. *Chem. Rev.* **1982**, *82*, 541.

(55) Bünzli, J.-C. G.; Piguet, C. *Chem. Rev.* **2002**, *102*, 1897.

(56) The TGA curve of **4** displayed weight losses between 30 and 150 °C—corresponding to 1.5 H_2O molecules (calcd 3.60%; found 3.41%)—and between 150 and 320 °C—corresponding to 0.4 DMF molecules (calcd 3.90%; found 4.07%). In the DTA curve, a small endothermic peak at 52 °C explained the loss of water molecules, while a large endothermic peak at 550 °C explained the collapse of the framework.

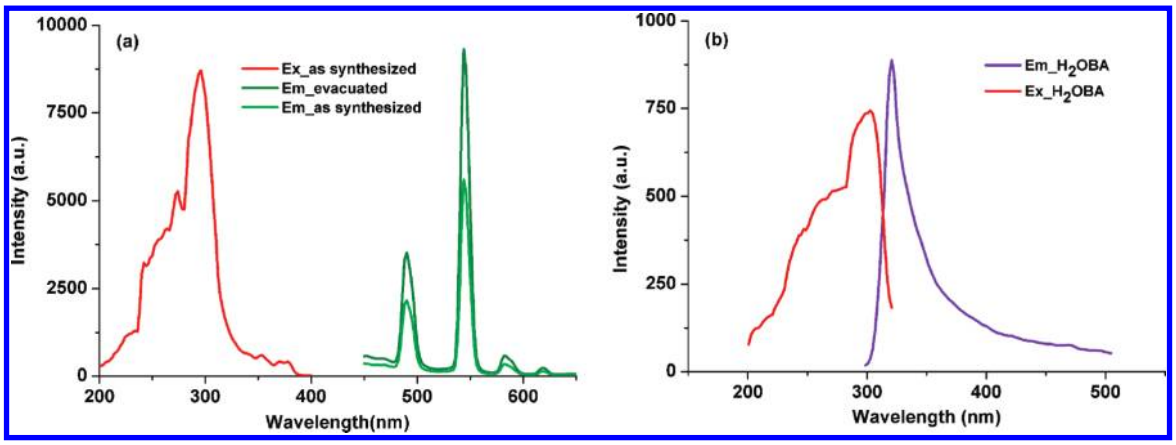

Figure 8. (a) Solid excitation and luminescence emission (excited at 295 nm) for as-synthesized **4**. The evacuated solid "Na[Tb(OBA)$_2$]" displays the stronger luminescence intensity. (b) Solid excitation and luminescence emission (excited at 275 nm) for H_2OBA.

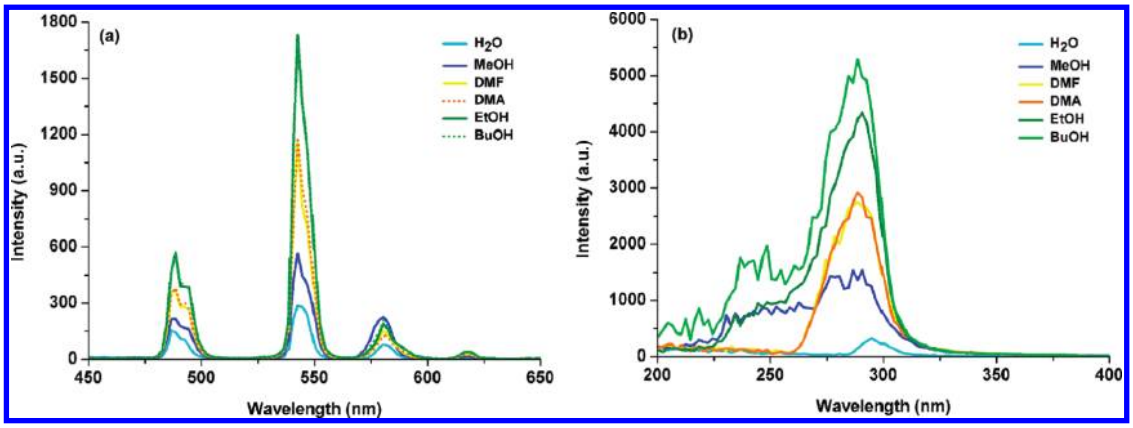

Figure 9. (a) Solution emission (excited at 295 nm) and (b) solution excitation spectra for powder "Na[Tb(OBA)$_2$]" dispersed in various solvents. Color scheme: H_2O, cyan; MeOH, blue; DMA, orange; DMF, yellow; EtOH, dark green; BuOH, green.

intensity of this evacuated solid clearly demonstrates the crystallinity of its framework and suggests its potential application as a luminescence probe[57] (Figure 8a).

The luminescence measurements of 5 mg "Na[Tb(OBA)$_2$]" dispersed in 2 mL solvents after 24 h clearly displayed that the $^5D_4 \rightarrow {}^7F_4$ emissions at 545 nm were the strongest intensities in BuOH and EtOH suspensions, but these intensities were significantly reduced in MeOH and H_2O suspensions (Figure 9a). The small molecules H_2O and MeOH could enter the coordination spheres of the terbium ions within the framework that quenches the luminescence intensities effectively.[54,55] The EtOH and BuOH molecules, which possess relatively sterically bulky alkyl groups, might protect the terbium ions from quenching by O−H oscillators. Interestingly, the sample did not display its strongest emission in a DMF suspension, unlike the sensing ability for the evacuated framework Eu(BTC) immersed in various solvents. We suspected that the different sizes and geometries of active metal centers exposed in these frameworks—six- and eight-coordinated metal sites in the evacuated Eu(BTC) and Na-[Tb(OBA)]$_2$ solids, respectively—could be an important reason for their own unique sensing abilities.[36,54] The samples dispersed in dimethyl acetamide (DMA) exhibited the same luminescence response as that in DMF. The excitation spectra of these suspensions show the relative intensities corresponding to their luminescence behavior (Figure 9b).

The powders after immersion in these solvents were recollected by filtration and dryed at the ambient temperature. The PXRD patterns of the samples filtered from MeOH and EtOH suspensions revealed that the evacuated framework may still retain the structural ordering as the original phase (Supporting Information, Figure S8). However, the pattern for the sample filtered from an H_2O suspension had the (110) reflection shifted slightly, the (330) reflection almost disappeared, and few small peaks emerged, which indicated that water molecules possibly entered the coordination sphere of terbium ions and then perturbed the crystal lattice of framework. This phenomenon might explain why the luminescence intensity was quenched so effectively through O−H oscillators in an H_2O suspension. The local geometry of the framework could be slightly affected by the introduction of DMF molecules because a few new peaks appeared in the PXRD pattern. The behavior of guest molecules adsorbed within the evacuated solid "Na[Tb(OBA)$_2$]" was further examined by the TGA curves of these filtered samples (Supporting Information, Figure S9). The curvatures displayed that MeOH or EtOH molecules adsorbed in the solids were evaporated completely before about 65 °C; whereas H_2O and DMF molecules were bound more tightly within the solids to be evaporated completely until about 180 and 300 °C, respectively. We therefore measured the luminescence for the evacuated solid "Na[Tb(OBA)$_2$]" after immersion in DMF and H_2O for 1 day. The solid luminescence spectra revealed

(57) Binnemans, K. *Chem. Rev.* **2009**, *109*, 4283.

that the metal centers exposed in the framework were active toward DMF and H_2O molecules displaying the increased and decreased intensity, respectively (Supporting Information, Figure S10).

Conclusion

We have used organic and inorganic cations as templates, often applied in the field of porous inorganic frameworks, to affect the formation of a complete system of lanthanide MOFs exhibiting rich structural chemistry. The solvent is also an important factor to cooperate with cationic templates to induce the phase formed. The third phase is a rare open framework precipitated with a late (Yb) and middle (Tb) lanthanide without the auxiliary ligands. Removal of the lattice molecules resulted in an inherently robust terbium-based open framework, which was active toward solvent molecules. This framework extends across the lanthanide series from europium to neodymium ions[58] (data not presented here), suggesting their potential application to metal-to-metal sensitizing luminescence behvaior.[10,13,14]

Acknowledgment. We thank the National Science Council of Taiwan for financial support (NSC 97-2113-M-006-006), the NSC High Valued Instrument Center for obtaining the elemental analyses, and NCKU for supporting the single-crystal X-ray diffractometer.

Supporting Information Available: Crystallographic data for **1**−**4** in CIF format, an ORTEP drawing for **4**, TG/DTA curves for **1** and **2**, PXRD patterns for **3** and **4**, and luminescence spectra for **4**. This material is available free of charge via the Internet at http://pubs.acs.org.

(58) Crystal data for $Na[Eu(OBA)_2]\cdot L$: orthorhombic $Cmc2_1$, a = 26.947(3), b = 15.292(2), c = 7.2835(7) Å, V = 3001.4(6) Å^3, Z = 4, ρ = 1.521 g cm^{-3}, μ = 2.155 mm^{-1}, T = 293 K, 11424 total reflections, 3785 unique reflections (R_{int} = 0.0308), R_1 = 0.0577 [$I > 2\sigma(I)$], $wR2$ = 0.1750 [$I > 2\sigma(I)$]. Crystal data for $Na[Nd(OBA)_2]\cdot L$: orthorhombic $Cmc2_1$, a = 27.124(3), b = 14.991(1), c = 7.3606(5) Å, V = 2992.2(4) Å^3, Z = 4, ρ = 1.508 g cm^{-3}, μ = 1.801 mm^{-1}, T = 293 K, 11423 total reflections, 3297 unique reflections (R_{int} = 0.0491), R_1 = 0.0695 [$I > 2\sigma(I)$], wR_2 = 0.1943 [$I > 2\sigma(I)$].